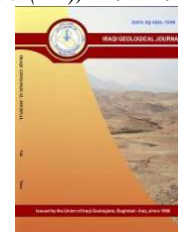




# Iraqi Geological Journal

Journal homepage: <https://www.igi-iraq.org>



## Liquefaction Characteristics of Sandy Soil Distributed in Wind Power Farms, Soc Trang Province, Vietnam

Nguyen Van Phong<sup>1</sup>, Nguyen Thanh Duong<sup>1,\*</sup> and Bui Truong Son<sup>1</sup>

<sup>1</sup> Hanoi University of Mining and Geology, Vietnam

\* Correspondence: [nguyenthanhduong@hmg.edu.vn](mailto:nguyenthanhduong@hmg.edu.vn)

### Abstract

Received:  
18 January 2022

Accepted:  
11 August 2022

Published:  
30 November 2022

Wind power has been widely utilized and has become a safe and renewable energy source in many countries. In Vietnam, many wind power farms have been built in coastal provinces such as Soc Trang, Bac Lieu, Ninh Thuan, Binh Thuan, Ca Mau, Vung Tau, and the Central Highlands. For onshore wind power farms, the dynamic loads generated from wind and the operation of the turbine will act on soil ground and affect the long-term strength and liquefaction potential of soil, especially for sandy soil. Thus, it is necessary to investigate the potential for liquefaction of the sandy soil layer in wind power farms. In this study, the liquefaction potential of sand distributed in onshore wind power farms in Soc Trang province, Vietnam was evaluated using the undrained cyclic triaxial test. The sand specimens were remolded using dry pluviation and moist tamping methods to simulate the field density. The analysis of test results showed that the very fine sand with a loose state distributed at the depth of less than or equal to 11.5 m could be liquefied under the testing conditions. While the fine sand specimens with a dense to very dense state distributed deeper than 30 m were not liquefied under testing conditions. However, for these specimens, the pore water ratio could be increased by 11.3 to 18.6% and this increase can lead to a decrease in soil strength.

**Keywords:** liquefaction; Cyclic triaxial test; Pore water pressure ratio; Wind power farms

## 1. Introduction

Wind energy is safe and renewable energy which has been widely utilized for the economic growth demand in many countries (Zheng et al., 2016). One of the biggest challenges when building a wind turbine is the impact of dynamic and cyclic loads on the foundation. For onshore wind turbines, the cyclic and dynamic loads acting on the foundations generate from wind, 1P (rotor frequency), and 2P/3P (blade passing frequency) (Nikitas et al., 2017). The soil properties such as long-term strength, and liquefaction potential can be changed under these loads and affects the long-term stability of wind turbine. In general, the cyclic strength and soil liquefaction potential can be indirectly evaluated based on the results of in-situ tests such as cone penetration test (SPT) (Seed and Idriss, 1971; Seed and Peacock, 1971; Iwasaki et al., 1982), cone penetration test (CPT) (Robertson and Wride, 1998; Ateş et al., 2014; Du et al., 2019), shear wave velocity ( $V_s$ ) (Hatanaka et al., 1997; Tokimatsu et al., 1986;

DOI: [10.46717/igi.55.2E.15ms-2022-11-29](https://doi.org/10.46717/igi.55.2E.15ms-2022-11-29)

Andrus and Stokoe, 2000; Ateş et al., 2014) or directly assessed based on laboratory tests such as cyclic triaxial test, cyclic direct simple shear test, cyclic torsional shear test, and shake table test (Satyam, 2012). Regarding the design of wind turbine foundations, the soil properties under dynamic and cyclic loads have been widely investigated (Safinur et al., 2011; Sim et al., 2013; Blaker and Andersen, 2019). In general, these studies have indicated the important role of laboratory testing to determine the cyclic properties of soil for designing turbine foundations.

In Vietnam, many wind power farms have been recently built and will be built in near future, especially in some provinces such as Soc Trang, Bac Lieu, Ninh Thuan, Binh Thuan, Ca Mau, Vung Tau, and the Central Highlands. According to the survey, Soc Trang's coastal areas have a great opportunity for wind power development since there is a plentiful and stable wind blowing every month of the year with the average wind speed at the height of 60 m between 6.2 to 6.4 m per second. According to the Ministry of Industry and Trade of Vietnam, 35740 hectares of land area in Soc Trang province has been investigated for wind power development with a potential capacity of 1470MW. The wind farm will be mainly distributed in three areas along the coastline, including Vinh Chau town, Tran De, and Cu Lao Dung districts. The planning areas of wind farms in Soc Trang province are mainly located on alluvial ground aged Holocene and Pleistocene. In which, the alluvial and marine sandy soils are common and distributed at different depths (Nu, 2014; Nu et al., 2020). These soils are sensitive to cyclic and dynamic loads, especially sandy soils. In which, the potential of soil liquefaction and reduction of soil shear strength under these loads is high and affects the stability of the foundation. Thus, investigation of the liquefaction potential of sandy soils in Soc Trang's coastal area is very important for ensuring the stability of the wind turbine foundation.

In Vietnam, the research on cyclic strength and soil liquefaction potential is still limited. Some of the previous studies regarding these issues are mostly focused on soils distributed in big cities such as Ha Noi and Ho Chi Minh cities (Binh et al., 2016; Phong, 2016; Phong and Thang, 2014, 2016). Recently, Nu et al. (2021) investigated the liquefaction potential of sandy soils in the North Central Coast of Vietnam based on SPT values. In general, these studies are mainly evaluated based on earthquake-induced liquefaction. However, the dynamic load generated from wind turbine operation is different from earthquakes. Besides, there has been no research on cyclic strength and the potential for liquefaction of sandy soil distributed in wind power farms in Vietnam. In this study, the sandy soil samples taken from boreholes in Vinh Chau town, Soc Trang province will be used to assess the liquefaction potential under dynamic loads generated from wind turbine operation. The undrained cyclic triaxial apparatus will be employed to investigate the liquefaction potential of sandy soil. For sandy soil, it is difficult to take the undisturbed soil samples, so the remolded samples which simulate the field density of sandy soils were prepared for the cyclic triaxial test.

## **2. Sample Preparation and Testing Procedure**

### **2.1. Sample Preparation**

Sandy soil samples were taken from two boreholes (S1, S2) in two wind farms in Vinh Chau town, Soc Trang province. Borehole S1 (coordinates: X=615930; Y=1034064) is located in Lac Hoa wind power farm whereas S2 (coordinates: X=617345; Y=1040603) is located in Hoa Dong wind power farm. The location of two boreholes for soil sampling is shown in Fig. 1.



**Fig. 1.** Location of soil sampling points

According to the documents of geotechnical investigation, there are two types of sand distributed in the study area to the depth of 55m (S1) and 60m (S2). The characteristics of sand layers in two boreholes are listed in Table 1. As shown in this table, the sand layers are distributed alternating with clayey soft soil layers. In which, the very fine sand layer (layer 2) with a loose state is distributed from 2.5 to 13.0 m while the fine sand with a dense (layer 5) to a very dense state (layer 6) is distributed from 31.0 to 60.0 m. The average thickness of layer 2 is 3.5m whereas the average thickness of layers 5 and 6 is 8.0m and 10.0m, respectively. The standard penetration resistance ( $N_{SPT}$ ) is from 3 to 5 blows for layer 2; from 27 to 42 blows for layer 5, and above 50 blows for layer 6. Based on the field description of sand samples, the SPT values, and the results of particle analysis, it is seen that the sand layers in two boreholes (S1, S2) are almost identical. The underground water levels recorded in two boreholes varied from 1.0 to 1.6 m.

**Table 1.** Characteristics of sand layers distributed in the study area (Phong, 2020)

Soil layer	Distribution depth (m)		Average thickness (m)	Sand types	$N_{SPT}$ (Blows)
	Layer surface	Layer bottom			
1	0	2.5 (S1)-5.0 (S2)	3.5	Mud clay	1
2	2.5-5.0	9.0 (S1)-13.0 (S2)	6.0	Very fine sand, loose state	3-5
3	9.0-13.0	20.0 (S1)-25.0 (S2)	13.0	Mud sandy clay	1
4	20.0-25.0	31.0 (S1)-45.0 (S2)	20.0	Sandy clay	4-6
5	31.0-45.0	45.5 (S1)-50.0 (S2)	8.0	Fine sand, dense state	27-42
6	45.5-50.0	55.0 (S1)-60.0 (S2)	10.0	Fine sand, very dense state	>50

Sand samples will be taken from 3 sand layers (Nos. 2, 5, 6) for this investigation. Since the sand layers in two boreholes are almost similar, sand samples in each layer of two boreholes were well mixed for sample preparation. The sand mixture samples are denoted as C1, C2, and C3. Some physical properties of these sand samples are presented in Table 2. As shown, the maximum void ratios of tested sand samples are from 1.021 to 1.050 while the minimum void ratios range from 0.577 to 0.593.

**Table 2.** Some physical properties of tested sand samples (Phong, 2020)

Sand samples	Grain size			Specific density (g/cm <sup>3</sup> )	Maximum void ratio	Minimum void ratio
	D <sub>60</sub> (mm)	D <sub>30</sub> (mm)	D <sub>10</sub> (mm)	$\gamma_s$	$e_{max}$	$e_{min}$
C1 – Layer 2	0.28	0.14	0.06	2.65	1.021	0.577
C2 – Layer 5	0.35	0.23	0.10	2.65	1.050	0.589
C3 – Layer 6	0.36	0.24	0.12	2.65	1.040	0.593



**Fig. 2.** Split mold and sand specimen for cyclic triaxial test

For sandy soil, the specimens for laboratory testing can be prepared according to four methods: dry and wet pluviations, and dry and moist tamping (Mulilis et al., 1976; Juneja and Raghunandan, 2008, 2010). The dry and wet pluviations, and dry tamping methods often produce specimens with a low density (high void ratio) (Juneja and Raghunandan, 2010). In this study, sand sample C1 was taken from the loose sand layer (layer 2), so the dry pluviation method will be employed for sample preparation. The sand samples C2, and C3 were taken from dense to very dense sand layers (layers 5 and 6), so the moist tamping method may be suitable for sample preparation of these sand samples. In the dry pluviation method, the dry sand is poured into the split mold with an inner diameter of 70 mm and a height of 140 mm (Fig. 2) using a pluviator device. The density of the sample is controlled by the amount of dry sand pouring into the mold. In the moist tamping method, after determining the amount of dry sand based on the desired density, it will be mixed with de-aired water at a moist content of 2%. To

ensure a uniform density of the sample, the amount of dry sand will be divided into seven equal parts. Each part is well mixed with de-aired water to the moist content of 2% and then placed into a split mold by the spoon and carefully compacted at a fixed height of 20 mm (the total height of 140 mm). The remold sample after preparation is shown in Fig. 2. In this study, sand samples will be remolded using the methods mentioned above to simulate different distribution depths, especially for sand in shallow depths such as layer 2. Some properties of sand specimens before testing are listed in Table 3. As presented in this table, initial relative density ( $D_r$ ) of samples C1 represented for layer 2 (loose state) ranges from 0.180 to 0.287. For sand samples C2, and C3 (represented for layers 5 and 6), the values of  $D_r$  range from 0.643 to 0.790.

**Table 3.** Properties of sand specimens used in this study (Phong, 2020)

Sample	Simulated depth (m)	Sample preparation method	Size of specimen (mm)		Dry density (g/cm <sup>3</sup> )	Initial void ratio	Initial relative density
			Diameter, D	Height H	$\gamma_c$	$e_0$	$D_r$
C1-0	8.5	Dry pluviation	70.0	140.8	1.377	0.936	0.189
C1-1	5.8	Dry pluviation	70.0	141.5	1.402	0.897	0.277
C1-2	7.0	Dry pluviation	70.0	140.0	1.420	0.893	0.287
C1-3	11.5	Dry pluviation	69.8	139.6	1.442	0.895	0.282
C1-4	7.0	Dry pluviation	70.0	140.0	1.376	0.937	0.188
C2-1	34.0	Moist tamping	70.5	141.0	1.572	0.692	0.777
C2-2	43.0	Moist tamping	69.3	140.0	1.572	0.686	0.790
C2-3	31.5	Moist tamping	71.0	139.5	1.518	0.753	0.643
C3	43.0	Moist tamping	69.3	139.7	1.549	0.711	0.736

## 2.2. Testing Procedure

The cyclic triaxial test apparatus (Tritech 50 KN – Controls Group) is employed for this investigation. The testing procedure was conducted in accordance with ASTM D5311 (ASTM-D5311, 2013) and included three main stages: saturation, consolidation, and cyclic loading. For the saturation stage, the back-pressure saturation method is used to saturate the sand specimens in this study. The difference in cell and back pressures is maintained at 10 kPa. The saturation of the specimen is confirmed based on Skempton's B-parameter. It is the ratio of the change in pore water pressure  $\Delta u$  to a change in cell pressure  $\Delta \sigma_c$  in an undrained condition. The saturation process is completed when the B value is higher or equal to 0.95. Normally, the full saturation of very fine sand was obtained with a back pressure of 70 kPa.

For the consolidation stage, after the saturation condition of the specimen has been obtained, the specimen was consolidated under the effective confining pressure at which it would be tested. The consolidation process was conducted by increasing the cell pressure to the desired value and then opening the valve for drainage. The cell pressure was increased to reach the desired effective confining pressure which is the difference between the cell and back pressures. To simulate the field condition, the effective confining pressure will be set equal to the effective overburden pressure which is based on the simulated depth of samples and water table level. The parameters for saturation and consolidation stages are shown in Table 4.

**Table 4.** Parameters for saturation and consolidation stages (Phong, 2020)

Sample	Simulated depth (m)	Saturation		Consolidation		
		$\sigma_{cell}$ (kPa)	$\sigma_{back}$ (kPa)	$\sigma_{cell}$ (kPa)	$\sigma_{back}$ (kPa)	$\sigma'_c$ (kPa)
C1-0	8.5	90	80	140	80	60
C1-1	5.8	100	90	120	80	40
C1-2	7.0	80	70	120	70	50
C1-3	11.5	100	90	160	80	80
C1-4	7.0	80	70	120	70	50
C2-1	34.0	90	80	320	80	240
C2-2	43.0	110	100	400	100	300
C2-3	31.5	90	80	300	80	220
C3	43.0	210	200	500	200	300

For the cyclic loading stage, the testing parameters were chosen based on types of construction works and dynamic loads. For the onshore wind power farms, the load caused by wind and operation of the turbine is cyclic and acts on the foundation for a long time, so the number of cycles required is high. The frequency ( $f$ ) is often chosen in the range of 0.4 to 1 Hz (Bhattacharya, 2019). In this study, the frequency of 1 Hz will be applied throughout the tests. The stress amplitude ( $\Delta\sigma_a$ ) was determined based on the desired cyclic stress ratio (CSR) as the following formula:  $\Delta\sigma_a = CSR \times 2\sigma'_c$  ( $\sigma'_c$ : effective isotropic consolidation stress). The CSR can be determined based on two conditions: 1) Utilizing the maximum bearing capacity of the soil ( $CSR_{ult}$ ), in this case, the  $CSR_{ult}$  can be estimated based on  $N_{spt}$  values; 2) According to the maximum stress value that the construction load is likely to cause in the ground. Under this condition, the greater the depth, the smaller the CSR values.

### 3. Results and Discussions

After completing the consolidation stage, the cyclic loading for all specimens was conducted with the same frequency of 1 Hz with different CSR values. The specimens at shallow depths and close to the dynamic source will have a high value of CSR and vice versa. The test results of 9 sand specimens are summarized in Table 5.

As shown in Table 5, the very fine sand specimens (C1-0, C1-1, C1-2, C1-3, and C1-4) are distributed from 5.5 to 11.5m having a relative density of lower or equal to 0.3 (loose state) whereas the fine sand specimens (C2-0, C2-1, C2-2, C3) are distributed at the depth of higher than 30m having the relative density greater than 0.7 (dense state). It can be seen that these results are consistent with the field conditions of these sand specimens. The results of the cyclic triaxial test on some sand specimens C1-2 (liquefied) and C2-1 (non-liquefied) are shown in Figs. 3 and 4, respectively. As shown in Fig. 4a, the pore pressure ratio ( $R_u$ ) significantly increases in the first 15 cycles (increasing in density), after that it will increase to about 70% at the cycle of 225. Above 70%,  $R_u$  quickly increases and reaches 100% at the cycle of 228. The changes in stress and strain are insignificant with  $R_u$  of less than 70%. When  $R_u$  increases above 70%, the stress decreases while the strain increases significantly and exceeds 5% (Fig. 5a). This sand specimen is liquefied at the cycle of 228. The cyclic behavior of other sand specimens at layer 2 (C1-0, C1-1, C1-3, C1-4) is also similar to that of the sand specimen C1-2. For sand specimen C2-1, as shown in Fig. 4b, the values of  $R_u$  increase slowly with the increasing of cycles and reaches the value of about 18.6% at the cycle of 500. The strain as presented in Fig. 5b, significantly increases at about the first 100 cycles, then it slowly increases to about 0.5% at the cycle of 500. This sand sample is non-liquefied and its behavior is similar to that of sand specimens C2-0, C2-3, and C3.

**Table 5.** Summary of cyclic triaxial test results (Phong, 2020)

Specimen	Relative density after consolidation, $D_{rc}$	CSR	Stress amplitude (kPa)	Maximum strain (%)	Pore pressure ratio ( $R_u$ )					Liquefied cycles (Cycles)
					5 cycles (%)	50 cycles (%)	100 cycles (%)	200 cycles (%)	Maximum (%)	
C1-0	0.192	0.234	28	7.86	100	-	-	-	100	4
C1-1	0.280	0.225	18	8.44	8.1	31.9	67.7	100.0	100	104
C1-2	0.290	0.200	29	6.46	8.0	25.4	34.0	51.8	100	228
C1-3	0.300	0.181	20	5.94	3.4	22.6	30.8	45.1	100	298
C1-4	0.191	0.160	16	4.72	24.2	64.2	77.4	88.8	100	468
C2-0	0.780	0.230	55	0.13	7.43	12.1	13.4	14.8	16.7	$\infty$
C2-1	0.794	0.100	60	0.53	3.9	9.6	11.90	14.6	18.6	$\infty$
C2-2	0.701	0.095	38	0.87	8.7	11.5	12.6	13.6	15.0	$\infty$
C3	0.740	0.083	50	0.11	3.4	7.13	8.40	9.67	11.3	$\infty$

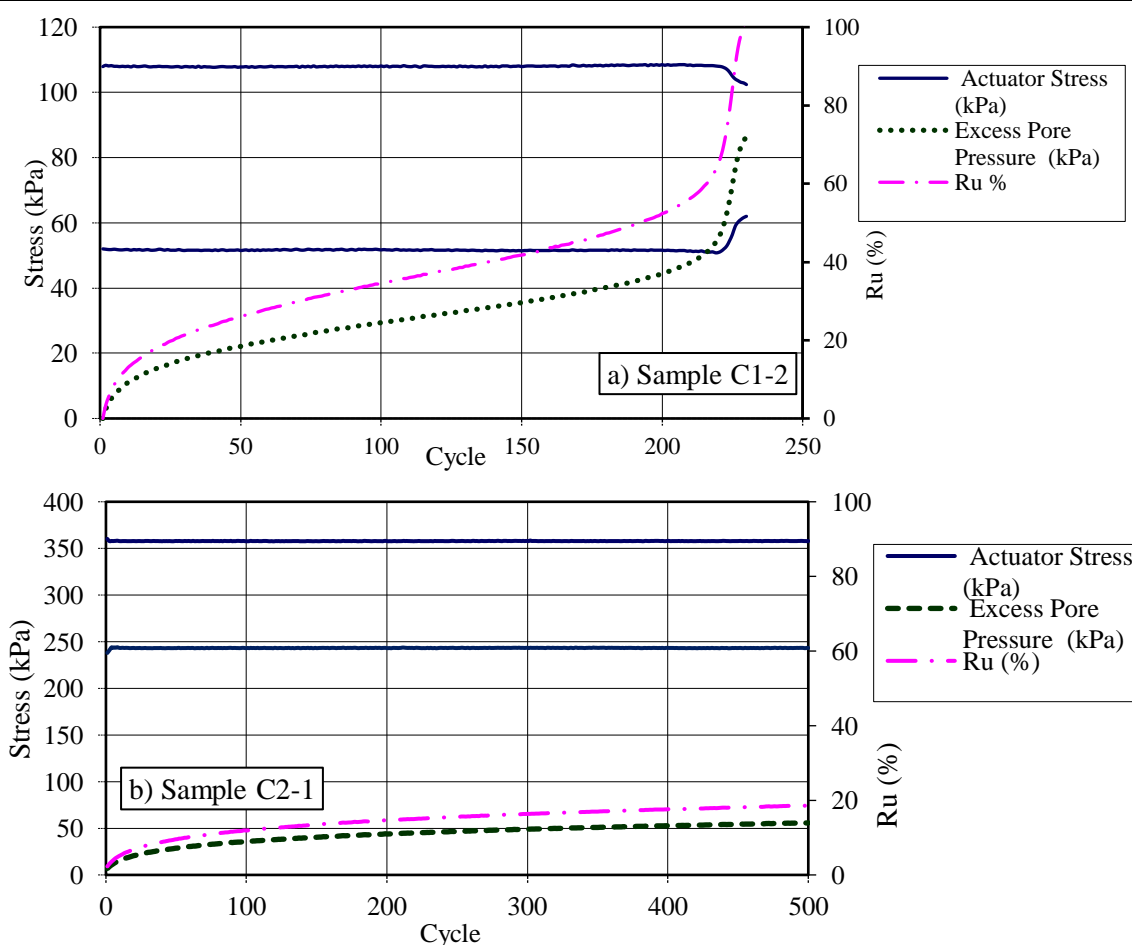


**Fig. 3.** Relationship between stress and cycles: a) sample C1-2; b) sample C2-1

In the case of liquefied failure, as shown in Fig. 3a, when  $R_u$  increases to higher than 60-70%, there is a significant change in stress and strain. However, the liquefied cycles, the level of strain, and the increase of  $R_u$  in different specimens are different since the values of CSR applied for these specimens are different. Fig. 5 presents the relationship between  $R_u$  and the value of CSR. It can be seen that the changes of  $R_u$  during cyclic loading significantly depend on the CSR. The higher CSR value, the faster  $R_u$  increases, especially at CSR above 0.2 and the specimen is prone to liquefy (specimen liquefies at a smaller number of cycles). As presented in Table 4, when the CSR values increase from 0.16 to 0.234, the liquefied cycles decrease from 468 to 4 cycles. As shown in Tables 4 and 5, in the study area, the sand distributed at the depth of less than or equal to 11.5 m will be liquefied under the

testing conditions. This result is consistent with that of previous studies. Satyam (2012) reported that the sand distributed deeper than about 15m is rarely found to be liquefied.

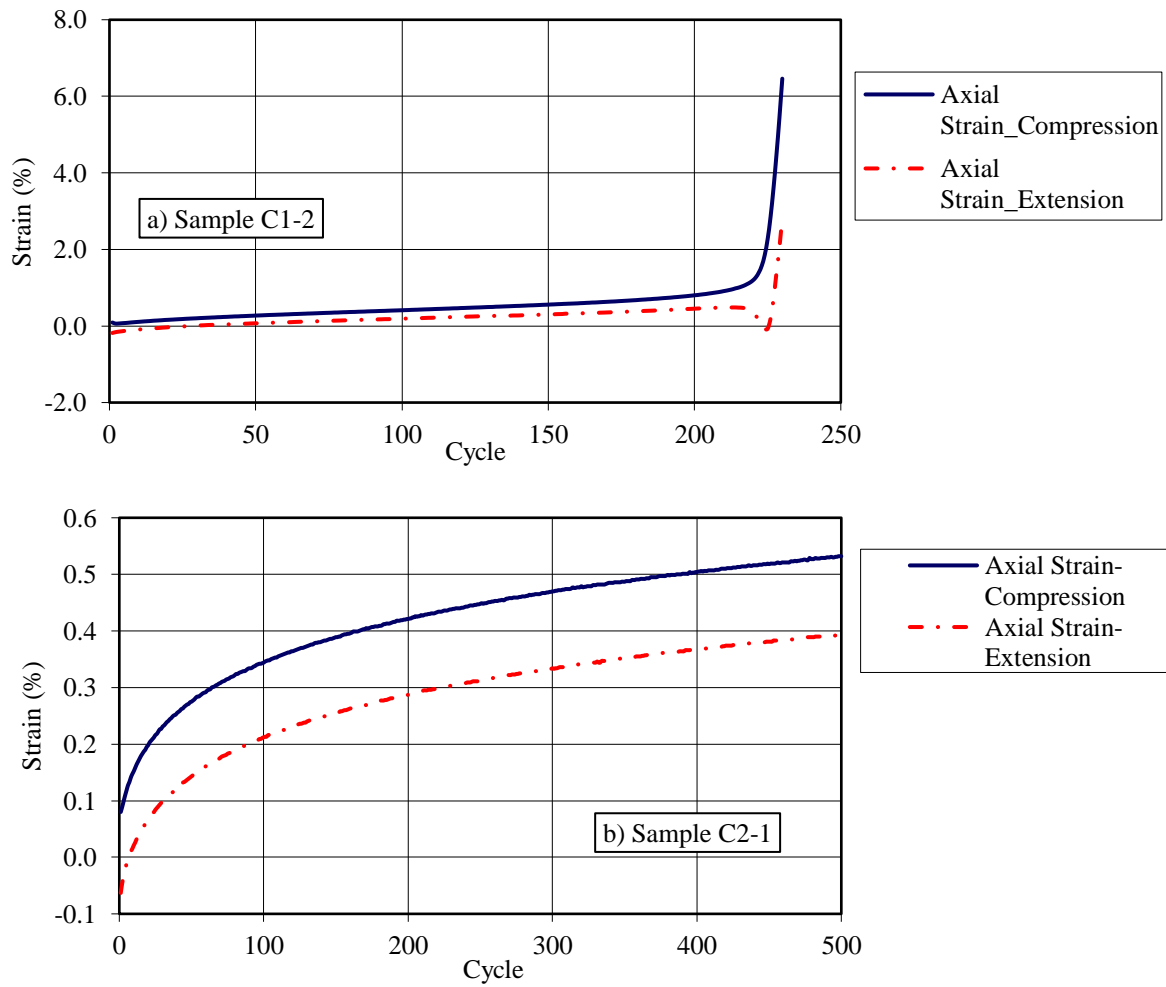


Fig. 4. Relationship between strain and cycles: a) a) sample C1-2; b) sample C2-1

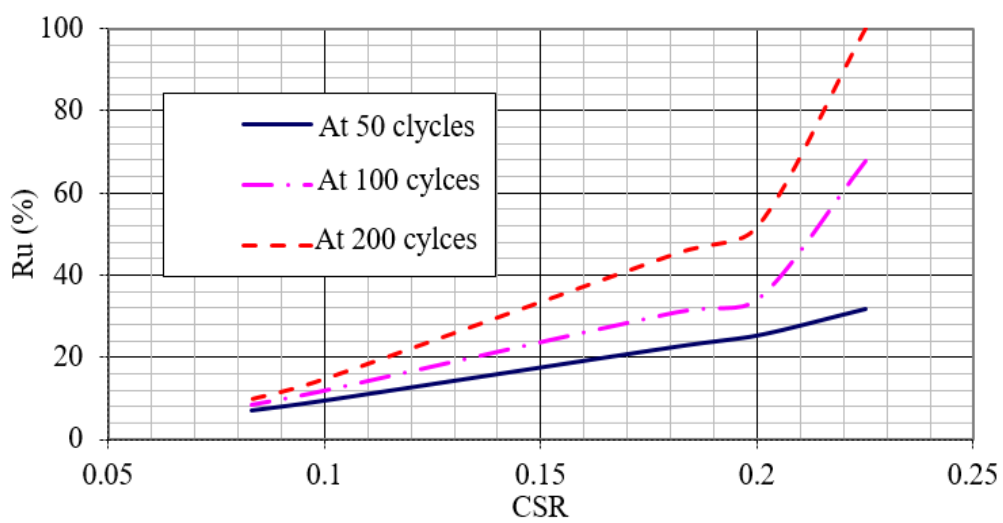
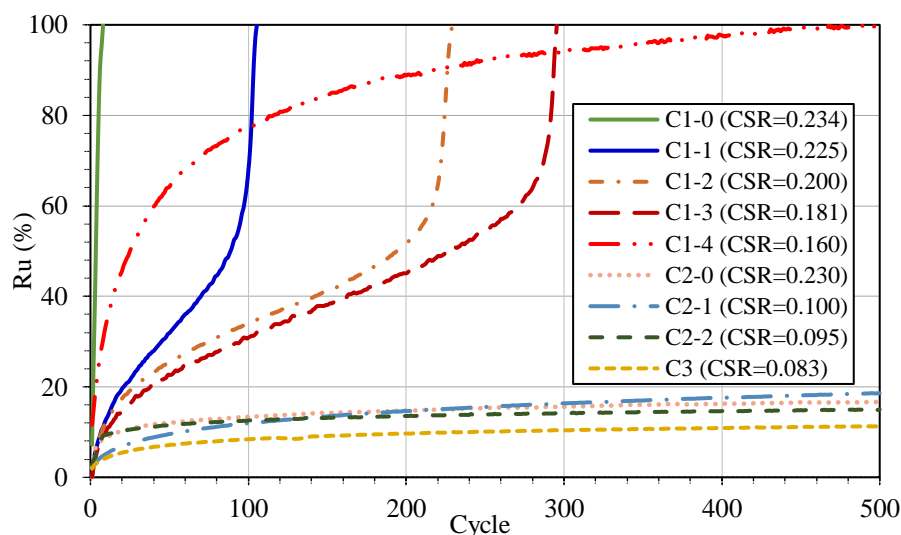


Fig. 5. Variation of  $R_u$  at different CSR values





**Fig. 6.** Change of  $R_u$  with the increase of cycles

The changes of  $R_u$  with the increase of cycles for different sand specimens are plotted in Fig. 6. As shown, there is a significant difference in  $R_u$  tendency between very fine sand specimens (C1-0, C1-1, C1-2, C1-3, C1-4) and fine sand specimens (C2-0, C2-1, C2-3, C3). For fine sand specimens distributed at a high depth, the CSR values are often less than or equal to 0.1. When the CSR is less than or equal to 0.1, the maximum increase of  $R_u$  is about 18.6% and the maximum strain is about 0.87%. For these sands, when the CSR is 0.23, the increase in  $R_u$  and strain is not significant. Thus, the fine sand at the depth of above 30 m seems to not liquefy under the testing conditions. However, the increase of  $R_u$  by 18.6% in fine sand can lead to a decrease in soil strength and affects the stability of the foundation when this sand is used as the bearing layer, especially for the pile foundations. Wada (2016) reported that in fine-grained soil, the excess pore water pressure generated at the pile toe during driving work could decrease the bearing capacity of the pile foundation. Therefore, the generation of excess pore water pressure in fine-grained soil under dynamic loads should be considered when estimating the bearing capacity of pile foundations.

#### 4. Conclusions

Based on the analysis of cyclic triaxial test results, some conclusions are drawn as follows:

- In the study area, the very fine sand distributed at less than or equal to 11.5m will be liquefied under the testing conditions. The liquefied cycles depend on the CSR values; it decreases from 468 cycles to 4 cycles when the CSR values increase from 0.16 to 0.234. Additionally, when the  $R_u$  increases to above 70%, the sand specimens will be quickly liquefied.
- For the dense fine sand above 30.0 m, it will not be liquefied under the testing conditions. However, the increase of  $R_u$  by 18.6% can decrease the soil strength and affects the bearing capacity of the foundation, especially for the pile foundation. Thus, the increase of pore water pressure under the dynamic loading should be considered when estimating the bearing capacity of the pile foundation.

#### Acknowledgements

The authors also would like to thank the staff at the Department of Engineering Geology and the lab of Geotechnical Engineering of Hanoi University of Mining and Geology for their help during conducting the experiments.

## References

- Andrus, R.D., Stokoe, K.H., 2000. Liquefaction resistance of soils from shear-wave velocity. *Journal of Geotechnical and Geoenvironmental Engineering* 126, 1015–1025.
- ASTM-D5311, 2013. Standard test method for load controlled cyclic triaxial strength of soil. *Annual Book of ASTM* 11.
- Ateş, A., Keskin, I., Totic, E., Yeşil, B., 2014. Investigation of soil liquefaction potential around efteni lake in Duzce Turkey: Using empirical relationships between shear wave velocity and SPT blow count (N). *Advances in Materials Science and Engineering*, 1-15.
- Bhattacharya, S., 2019. Design of foundations for offshore wind turbines. Wiley Online Library.
- Binh, V.B., Dung, N.N., Duong, T.N., Hai, H.P., Hung, V.N., 2016. The effect of frequency and effective consolidation stress on liquefaction potential of alluvial sand of Thai Binh Formation (aQ2-3tb1) in cyclic triaxial experiment. *Journal of Mining and Earth Sciences*, 31–37.
- Blaker, Ø., Andersen, K.H., 2019. Cyclic properties of dense to very dense silica sand. *Soils and Foundations*, 59, 982–1000.
- Du, G., Gao, C., Liu, S., Guo, Q., Luo, T., 2019. Evaluation method for the liquefaction potential using the standard penetration test value based on the CPTU soil behavior type index. *Advances in Civil Engineering* 2019.
- Hatanaka, M., Uchida, A., Ohara, J., 1997. Liquefaction characteristics of a gravelly fill liquefied during the 1995 Hyogo-Ken Nanbu earthquake. *Soils and Foundations*, 37, 107–115.
- Iwasaki, T., Tokida, K.I., Tatsuoka, F., Watanabe, S., Yasuda, S., Sato, H., 1982. Microzonation for soil liquefaction potential using simplified methods, in: *Proceedings of the 3rd International Conference on Microzonation*, Seattle, 1310–1330.
- Juneja, A., Raghunandan, M.E., 2010. Effect of sample preparation on strength of sands, in: *Indian Geotechnical Conference*, Mumbai, India, 327–330.
- Juneja, A., Raghunandan, M.E., 2008. Comparison of methods of sample preparation for triaxial tests on sands, in: *Proceedings of Indian Geotechnical Conference*, 14–17.
- Mulilis, J.P., Horz, R.C., Townsend, F.C., 1976. The effects of cyclic triaxial testing techniques on the liquefaction behavior of Monterey No. 0 sand. US Department of Defense, Department of the Army, Corps of Engineers
- Nikitas, G., Arany, L., Aingaran, S., Vimalan, J., Bhattacharya, S., 2017. Predicting long term performance of offshore wind turbines using cyclic simple shear apparatus. *Soil Dynamics and Earthquake Engineering*, 92, 678–683.
- Nu, N.T., 2014. Nghiên cứu đặc tính địa chất công trình của đất loại sét yếu amQ22-3 phân bố ở các tỉnh ven biển đồng bằng sông Cửu Long phục vụ xử lý nền đường. Doctoral thesis (In Vietnamese)
- Nu, N.T., Duong, N.T., Son, B.T., 2021. Assessment of Soil Liquefaction Potential Based on SPT Values at Some Ground Profiles in the North Central Coast of Vietnam. *Iraqi Journal of Science*, 2222–2238.
- Nu, N.T., Duong, N.T., Son, B.T., Thinh, P.H., 2020. Investigation of salt, alum content in soft soils and their effects on soil properties: Case study in coastal areas of Vietnam. *Iraqi Geological Journal*, 19–34.
- Phong, N.V., 2016. Nghiên cứu tính chất cơ học của trầm tích Đệ tứ phân bố ở khu vực Hà Nội dưới tác dụng của tải trọng động. Doctoral thesis (In Vietnamese).
- Phong, N.V., Thang, L.T., 2016. Research on liquefaction resistance of fine sand distributing in Hanoi by density. *International Conference on Geology and Geo-resources (ESASGD 2016)*, 174–178.
- Phong, N.V., Thang, L.T., 2014. Nghiên cứu độ bền động của một số loại đất yếu ở vùng ven biển Bắc Bộ bằng thí nghiệm ba trục động. Báo cáo tại Hội nghị KH Mô-Địa chất (In Vietnamese).
- Phong, N. V., 2020. Độ bền động và khả năng hóa lỏng của cát khu vực ven biển Sóc Trăng dưới tác dụng của tải trọng tuabin điện gió. Hội nghị Toàn quốc Khoa học trái đất và Tài nguyên với phát triển bền vững (ERSD, 2020), 85-91 (In Vietnamese)
- Robertson, P.K., Wride, C.E., 1998. Evaluating cyclic liquefaction potential using the cone penetration test. *Canadian Geotechnical Journal*, 35, 442–459.
- Safinus, S., Sedlacek, G. N, Hartwig, U., 2011. Cyclic response of granular subsoil under a gravity base foundation for offshore wind turbines, in: *International Conference on Offshore Mechanics and Arctic Engineering*, 875–882.

- Satyam, N., 2012. Review on liquefaction hazard assessment. *Advances in Geotechnical Earthquake Engineering, Soil Liquefaction and Seismic Safety of Dams and Monuments*, 63–82.
- Seed, H.B., Idriss, I.M., 1971. Simplified procedure for evaluating soil liquefaction potential. *Journal of Soil Mechanics & Foundations Div*, 1249-1273.
- Seed, H.B., Peacock, W.H., 1971. Test procedures for measuring soil liquefaction characteristics. *Journal of Soil Mechanics & Foundations Div*, 1099-1119.
- Sim, W.W., Aghakouchak, A., Jardine, R.J., 2013. Cyclic triaxial tests to aid offshore pile analysis and design. *Proceedings of the Institution of Civil Engineers-Geotechnical Engineering* 166, 111–121.
- Tokimatsu, K., Yamazaki, T., Yoshimi, Y., 1986. Soil liquefaction evaluations by elastic shear moduli. *Soils and Foundations*, 26, 25–35.
- Wada, A., 2016. Excess pore water pressure and its impact. *Japanese Geotechnical Society Special Publication*, 2, 335–339.
- Zheng, C.W., Li, C.Y., Pan, J., Liu, M.Y., Xia, L.L., 2016. An overview of global ocean wind energy resource evaluations. *Renewable and Sustainable Energy Reviews*, 53, 1240–1251.